ELSEVIER

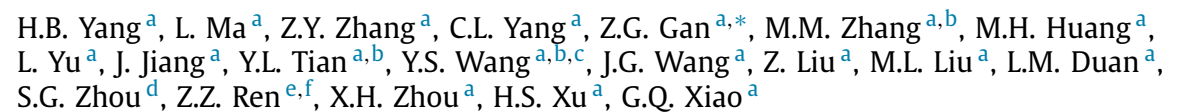
Contents lists available at ScienceDirect

### Physics Letters B

www.elsevier.com/locate/physletb



## Alpha decay properties of the semi-magic nucleus <sup>219</sup>Np





<sup>&</sup>lt;sup>b</sup> School of Physical Sciences, University of Chinese Academy of Sciences, Beijing 100049, China

#### ARTICLE INFO

# Article history: Received 18 September 2017 Received in revised form 24 November 2017 Accepted 6 December 2017 Available online 15 December 2017 Editor: V. Metag

Keywords: N = 126 shell closure Digital algorithm  $\alpha$ -particle energy Half-life Proton drip-line

#### ABSTRACT

The semi-magic nucleus  $^{219}$ Np was produced in the fusion reaction  $^{187}$ Re( $^{36}$ Ar,  $^{4}$ n) $^{219}$ Np at the gas-filled recoil separator SHANS (Spectrometer for Heavy Atoms and Nuclear Structure). A fast electronics system based on waveform digitizers was used in the data acquisition and the sampled pulses were processed by digital algorithms. The reaction products were identified using spatial and time correlations between the implants and subsequent  $\alpha$  decays. According to the observed  $\alpha$ -decay chain, an energy of  $E_{\alpha} = 9039(40)$  keV and a half-life of  $T_{1/2} = 0.15^{+0.72}_{-0.07}$  ms were determined for  $^{219}$ Np. The deduced proton binding energy of  $^{219}$ Np fits well into the systematics, which gives another evidence of that there is no sub-shell closure at Z = 92. The influence of the N = 126 shell closure on the stability of Np isotopes is discussed within the framework of  $\alpha$ -decay reduced widths.

© 2017 The Author(s). Published by Elsevier B.V. This is an open access article under the CC BY license (http://creativecommons.org/licenses/by/4.0/). Funded by SCOAP<sup>3</sup>.

#### 1. Introduction

Synthesis of neutron-deficient actinide nuclei close to the N=126 shell closure is of importance to understand the stability of the N=126 closed shell and to predict the limit of existence for nuclei in this region.  $\alpha$  decay is the dominant radioactive decay mode for these nuclei and  $\alpha$ -spectroscopic method has played crucial role to obtain information on nuclear structure and the evolution of N=126 neutron shell closure. In the past few decades, short lifetime and low production cross section are main difficulties in studying nuclei in this region. Thanks to the successful application of digital data acquisition systems [1,2] and the exploration on multinucleon transfer reactions [3,4], several new neutron-deficient actinide nuclei near N=126 neutron shell have been produced in recent years.

A recent work by J. Khuyagbaatar et al. [1] reported the discovery of a new short-lived isotope <sup>221</sup>U as well as unambiguous identification of <sup>222</sup>U. These two isotopes were produced in the fu-

sion reaction <sup>50</sup>Ti+<sup>176</sup>Yb at the gas-filled recoil separator TASCA and their decay properties were extracted from pileup traces by using software algorithms. Through the comparative analysis of the  $\alpha$ -decay reduced widths and the neutron-shell gaps of the Po-U isotopes, a significant weakening of influence of the N = 126 shell closure in U was observed. Most recently, M.D. Sun et al. [2] reported the discovery of the new short-lived isotope <sup>223</sup>Np, which was synthesized in the fusion reaction <sup>40</sup>Ar+<sup>187</sup>Re at the gas-filled recoil separator SHANS [5]. The  $\alpha$ -decay energy and half-life of <sup>223</sup>Np were also extracted from pileup traces recorded by a new digital data acquisition system. The systematics of proton separation energy together with the calculation of large-scale shell model gave a disproof of the existence of a Z = 92 shell gap, which was a prediction in systematic mean-field calculations [6] but was not supported by the subsequent theoretical calculations [7] and experimental works [8-10].

The discovery of new isotopes <sup>219</sup>Np, <sup>223</sup>Am, <sup>229</sup>Am and <sup>233</sup>Bk was reported by H.M. Devaraja et al. [3]. They were produced in the multi-nucleon transfer reaction of <sup>48</sup>Ca+<sup>248</sup>Cm and separated by the velocity filter SHIP at GSI. Beside the new isotopes about 100 further target-like transfer products were also identified, which indicate that multi-nucleon transfer reactions are promising

<sup>&</sup>lt;sup>c</sup> School of Nuclear Science and Technology, Lanzhou University, Lanzhou 730000, China

<sup>&</sup>lt;sup>d</sup> Institute of Theoretical Physics, Chinese Academy of Sciences, Beijing 100190, China

<sup>&</sup>lt;sup>e</sup> Department of Physics, Nanjing University, Nanjing 210093, China

f School of Physics Science and Engineering, Tongji University, Shanghai 200092, China

<sup>\*</sup> Corresponding author.

E-mail address: zggan@impcas.ac.cn (Z.G. Gan).

for the synthesis of new transuranium isotopes. However, due to the usage of traditional analog electronics, a few sum energies of pileup  $\alpha$  events were given, e.g., the decay events from  $^{223}\mathrm{Am}$  and  $^{225}\mathrm{Np}.$ 

These findings are very interesting and motivate us to carry out further investigations on the evolution of the N=126 shell closure beyond Z=92 and the possible ways to enter so far unknown regions in the upper part of the chart of nuclei. The isotones with N=126 have been reported up to  $^{219}{\rm Np}$  [3], however neither clear half-life nor clear decay energy of  $^{219}{\rm Np}$  was given. In this paper, we will report on the measurement of the  $\alpha$ -decay properties of  $^{219}{\rm Np}$  produced in the fusion reaction  $^{36}{\rm Ar}+^{187}{\rm Re}$ . Combining the measured data and some literature values, the absence of sub-shell closure at Z=92 and the weakening of the N=126 shell stabilization effect for Np will be discussed.

#### 2. Experimental setup and methods

The experiment was carried out at the gas-filled recoil separator SHANS [5] and a beam of  $^{36}$ Ar was delivered by the sector focusing cyclotron of the heavy ion research facility in Lanzhou (HIRFL), China. The incident beam energy was 191.5 MeV and the beam intensities were 300–400 pnA. The targets consisted of 380 µg/cm² thick layers of  $^{187}$ Re (enrichment 98.6%), which were evaporated on 45 µg/cm² thick carbon foils. The targets with the backing upstream were mounted on a stationary frame. The beam energy at the center of the target was estimated to be about 189.6 MeV using the program SRIM [11] and the total beam time was 155 hours.

The separator was filled with helium gas at a pressure of 0.6 mbar and the average charge state of <sup>219</sup>Np moving in the helium gas was estimated to be 6.7. The magnets of SHANS were set to guide the evaporation residue <sup>219</sup>Np with a magnetic rigidity of 1.77 Tm to the center of the focal plane with an estimated efficiency of 20%. The time of flight of the 219Np through separator was calculated to be 1.26(6) us. After filtering out by the separator, the evaporation residues (ERs) were implanted into three 300 µm thick position-sensitive strip detectors (PSSDs) installed side by side at the focal plane of the separator. Each PSSD, with an active area of  $50 \times 50 \text{ mm}^2$ , was divided into 16 vertical strips on the front face. Upstream the PSSDs, eight non-position-sensitive silicon detectors (side detectors) of the same type were mounted. The PSSDs and the side detectors formed a Si-box detector. The detection efficiency for  $\alpha$  decays of implanted nuclei was 80%. In order to distinguish the radioactive decay events of ERs from the implantation events, two multi-wire proportional counters (MW-PCs) were mounted 15 cm and 25 cm upstream from the PSSDs. The counter gas in two MWPCs was isobutane of 2.5 mbar pressure and the counter windows were made of 0.5 um Mylar.

After amplified with preamplifiers, signals of all detectors were processed in a digital data acquisition system. Sixteen 14-bits waveform digitizers V1724 [12] with 100 MHz sampling frequency developed by CAEN were used to record samples of the input signals and transfer them to FPGA (Field Programmable Gate Array) for real-time digital signal processing. The trapezoidal filtering algorithm [13] and the digital RC-CR<sup>2</sup> filter [14] implemented in the digitizer FPGA could convert the exponential signal from preamplifier into a trapezoidal signal and a bipolar RC-CR2 signal respectively. The amplitude of trapezoidal signal is proportional to the input pulse height and the zero crossing of RC-CR2 signal is independent of the pulse height. When the RC-CR<sup>2</sup> signal of PSSD or side detector exceeds the programmed threshold, a 15 µs-long trace of the input signal as well as the relevant amplitude and the time stamp calculated online were stored. So the recorded digital pulses can be reprocessed offline with different parameters or algorithms. While for each triggered pulse from MWPCs, only the amplitude of trapezoidal signal and the time stamp calculated in the FPGA were saved into the local memory buffer.

The offline digital signal processing was performed by using the data handling software ROOT [15]. Prior to the application of digital algorithms, a correlation among events from both ends of silicon strips, back of PSSDs, side detectors and MWPCs was made based on time stamps. The events from different detectors that can be correlated within the setting time windows were written into one entry. In order to facilitate searching for  $\alpha$ -decay chains in the next time, all entries were arranged in chronological order. For each trace correlated in one entry, the first 200 samples were used for baseline calculation. After subtracting the baseline, the two traces from the top and bottom of the silicon strip were added up as a complete trace taking into account the amplification factors of the preamplifiers. Then each complete trace with 1500 samples was analyzed by using a digital leading-edge discriminator [16] and the trapezoidal algorithm [13] to extract the time and the amplitude information respectively.

 $\alpha$ -particle energy calibrations were performed using a three-peak ( $^{244}$ Cm, $^{241}$ Am and  $^{239}$ Pu) external  $\alpha$  source as well as the known peaks from nuclei produced in the test reaction  $^{36}$ Ar+ $^{175}$ Lu [17]. Energy resolutions of individual strips of PSSDs were 60–70 keV (FWHM) for 6–10 MeV  $\alpha$  particles that were registered as single events in the traces. The vertical position of each event was determined by resistive charge division [18], and the position resolution of each silicon strip was better than 1.5 mm (FWHM).

#### 3. Experimental results

The identification of rare products were performed using a recoil- $\alpha$ - $\alpha$  correlation method. A two-dimensional plot showing the correlation between parent and daughter  $\alpha$ -particle energies of type ER- $\alpha_1$ - $\alpha_2$  is shown in Fig. 1. The analysis of the correlation was made with a vertical position window of  $\pm 1.5$  mm and the time windows of 30 ms for the ER- $\alpha_1$  pair and 20 s for the  $\alpha_1$ - $\alpha_2$  pair. In the plot some known isotopes produced in 1pxn, 2pxn and 3pxn fusion-evaporation channels such as  $^{218}$ U,  $^{214,215}$ Pa,  $^{217,218}$ Pa,  $^{213,214}$ Th can be recognized.

For  $^{218}$ U, three  $\alpha$ -decay chains associated with  $^{218g}$ U and two  $\alpha$ -decay chains associated with an isomeric state  $^{218m}$ U(8+) were identified. The  $\alpha$ -particle energies and half-lives were determined to be 8619(35) keV and  $0.131^{+0.179}_{-0.048}$  ms for  $^{218g}$ U and  $^{10685}$ (35) keV and  $0.134^{+0.244}_{-0.053}$  ms for  $^{218m}$ U. The determined  $\alpha$ -particle energies are in good agreement with the literature values  $E_{\alpha}(^{218g}$ U) = 8612(9) keV and  $E_{\alpha}(^{218m}$ U) = 10678(17) keV [9, 10]. However due to the low statistics, the determined half-lives are shorter than the reported values  $T_{1/2}(^{218g}$ U) =  $0.51^{+0.17}_{-0.10}$  ms and  $T_{1/2}(^{218m}$ U) =  $0.56^{+0.26}_{-0.14}$  ms [9,10]. Another correlation analysis has been performed for  $^{214,215}$ Pa. Twenty correlated  $\alpha$ -decay chains attributed to the  $\alpha$  decay of  $^{214,215}$ Pa were found. Based on these chains, an  $\alpha$ -particle energy of 8089(30) keV and a half-life of  $14.6^{+4.2}_{-2.7}$  ms were deduced for the mother activity, which are consistent with the reported decay properties of  $^{215}$ Pa ( $E_{\alpha}=8091(15)$  keV,  $T_{1/2}=14(2)$  ms) [19] and  $^{214}$ Pa ( $E_{\alpha}=8116(15)$  keV,  $T_{1/2}=17(3)$  ms) [19].

One four-member decay sequence suspected as the  $\alpha$  decay from <sup>219</sup>Np was observed and that can be found in the upper part of Fig. 1. Together with the measured energies, time intervals and vertical positions of each activity, the entire decay chain is shown in Fig. 2. All activities in the decay chain were detected during beam irradiation. Before the identification of this decay chain, the possibility  $P_{\rm err}$  that the observed event sequence arises from a

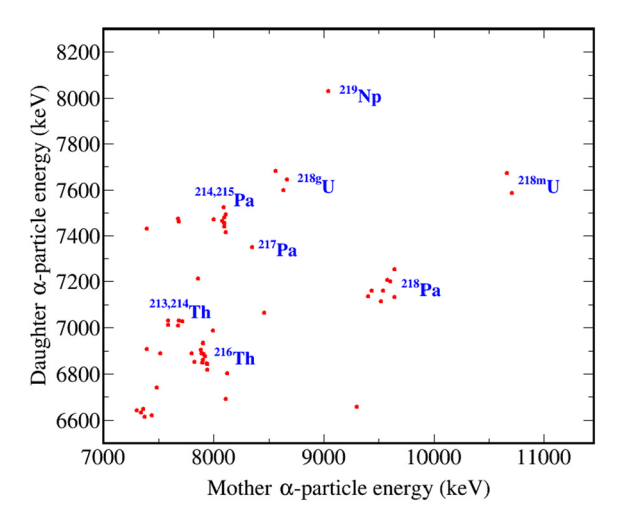


**Fig. 1.** (Color online.) Mother and daughter  $\alpha$ -particle energies for all chains of the type ER- $\alpha_1$ - $\alpha_2$  observed in the 191.5 MeV  $^{36}$ Ar+ $^{187}$ Re irradiation. Maximum search times were 30 ms for the ER- $\alpha_1$  pair and 20 s for the  $\alpha_1$ - $\alpha_2$  pair.

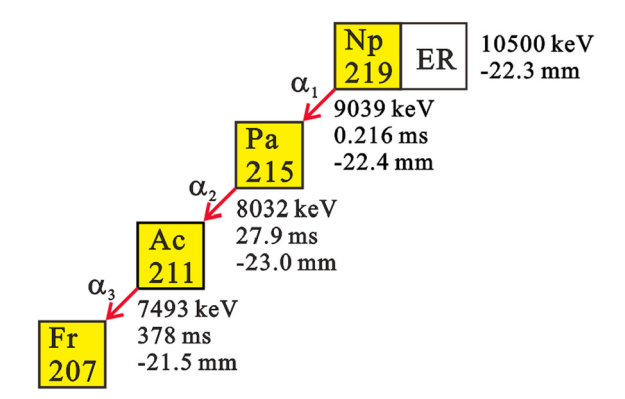


**Fig. 2.** (Color online.) The observed  $\alpha$ -decay chain assigned to  $^{219}$ Np. Experimental energies, time intervals and vertical positions of all activities are shown.

random correlation of unrelated events needs to be estimated. A method described in Ref. [18] was applied to calculate  $P_{err}$  on the basis of observed average counting rates in the detectors.  $P_{\rm err}$  was estimated to be less than  $3.8 \times 10^{-11}$  and the expected number of random decay chain was  $1.0 \times 10^{-4}$ . Thus this decay chain was considered to be a real correlation. The measured  $\alpha$ -particle energy and lifetime of the daughter activity are 8032 keV and 27.9 ms respectively and this decay can be recognized as the  $\alpha$  decay from  $^{214}$ Pa or  $^{215}$ Pa. The measured  $\alpha$ -particle energy of 7493 keV and lifetime of 378 ms for the granddaughter decay are consistent with the  $\alpha$  decay of  $^{210}$ Ac and  $^{211}$ Ac, whose reported  $\alpha$ decay properties are  $E_{\alpha} = 7462(8)$  keV,  $T_{1/2} = 350(40)$  ms [20] for <sup>210</sup>Ac and  $E_{\alpha} = 7477(6)$  keV,  $T_{1/2} = 210(30)$  ms [20] for <sup>211</sup>Ac, respectively. Therefore, the mother activity with measured  $\alpha$ -particle energy of 9039 keV and lifetime of 0.216 ms can be assigned to the  $\alpha$  decay of <sup>218</sup>Np or <sup>219</sup>Np. Systematic regularities of the experimental  $\alpha$ -decay energies and half-lives of neutron-deficient Ac-Np isotopes were shown in Fig. 3. According to the systematics, the ground state  $\alpha$ -decay properties of <sup>219</sup>Np and <sup>218</sup>Np will have significant differences in analogy with the  $\alpha$ -decay properties of the other known 126-neutron and 125-neutron isotopes such as <sup>218</sup>U and <sup>217</sup>U, <sup>217</sup>Pa and <sup>216</sup>Pa, <sup>216</sup>Th and <sup>215</sup>Th, <sup>215</sup>Ac and <sup>214</sup>Ac. A simple linear extrapolation of the  $\alpha$  energies of nuclei with N=126and N = 125 gives the estimated  $\alpha$ -particle energies of 9000(60) keV for <sup>219</sup>Np and 8580(60) keV for <sup>218</sup>Np. The measured energy 9039 keV is much close to the estimated  $\alpha$ -particle energy of  $^{219}$ Np. Therefore we prefer to assign this decay chain to the  $\alpha$ 

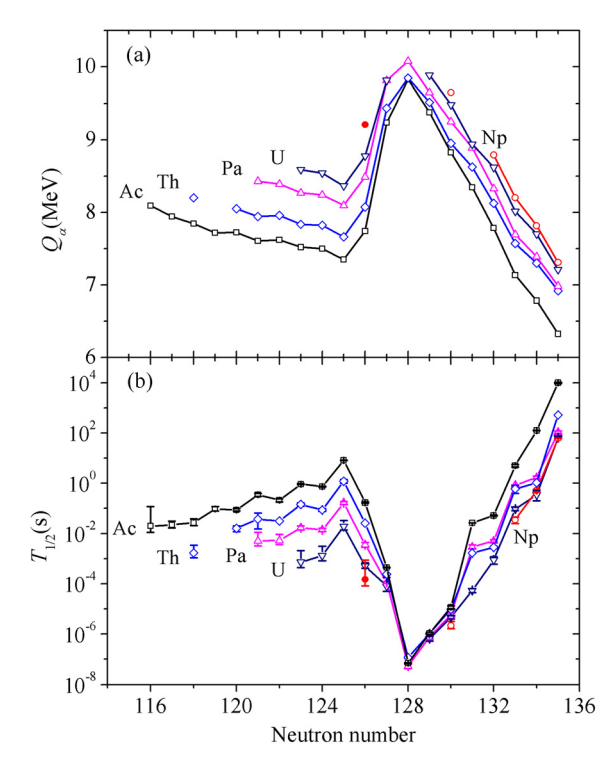


**Fig. 3.** (Color online.) (a)  $\alpha$ -decay energies  $Q_{\alpha}$  of ground state to ground state transitions and (b) half-lives  $T_{1/2}$  for neutron-deficient Ac, Th, Pa, U and Np isotopes as a function of neutron number. Here  $Q_{\alpha}=(1+m_{\alpha}/m_d)\times E_{\alpha}$ , where  $(m_{\alpha}/m_d)\times E_{\alpha}$  denotes the recoil energy of residual nucleus. Open symbols refer to literature values taken from Refs. [19,20,25]. The red solid circles refer to the values of  $^{219}$ Np measured in present work.

decay of ground state to ground state transition from  $^{219}\mathrm{Np}$  rather than  $^{218}\mathrm{Np}.$ 

Based on the observed decay chain, the  $\alpha$ -particle energy of <sup>219</sup>Np was determined to be 9039(40) keV. The error limits for the  $\alpha$ -particle energy were established from the quadratic sum of standard error (30 keV) and the energy calibration error (25 keV). To evaluate the half-life of <sup>219</sup>Np, the maximum likelihood method described in Ref. [21] was used. From the 0.216 ms ER- $\alpha_1$  time interval one can deduce the most probable half-life value of 0.15 ms and a half-life range of (0.08-0.87) ms. The indicated range corresponds to a 68.3% confidence level. In order to reproduce the half-life, the new Geiger-Nuttall law given in Refs. [22,23] relating half-life and  $\alpha$ -decay energy was used. The calculated half-life for <sup>219</sup>Np is 0.293 ms, which is consistent with the determined value of  $0.15^{+0.72}_{-0.07}$  ms. We also plotted the deduced  $\alpha$ -decay energy ( $Q_{\alpha} = 9207(40)$  keV) and half-life on Fig. 3. As can be seen, not only the deduced  $\alpha$ -decay energy but also the determined half-life fits well into the systematics. Using a transmission efficiency of 20%, the cross section for <sup>219</sup>Np at the beam energy of 191.5 MeV was determined to be  $19^{+44}_{-16}$  pb. The error bars of the cross section only represent statistical errors determined by the method described in Ref. [21].

#### 4. Discussion

According to the measured  $\alpha$ -decay energy of  $^{219}$ Np and the masses of  $^{215}$ Pa and  $^{218}$ U given in [24] a proton binding energy  $S_p = -301(83)$  keV and a ground state binding energy relative to  $^{208}$ Pb of 28928(81) keV were determined. Negative value of proton binding energy indicates that the proton drip-line for neptunium has been reached experimentally. As can be seen from Fig. 4(a), the proton binding energy of  $^{219}$ Np fits well into the systematics and

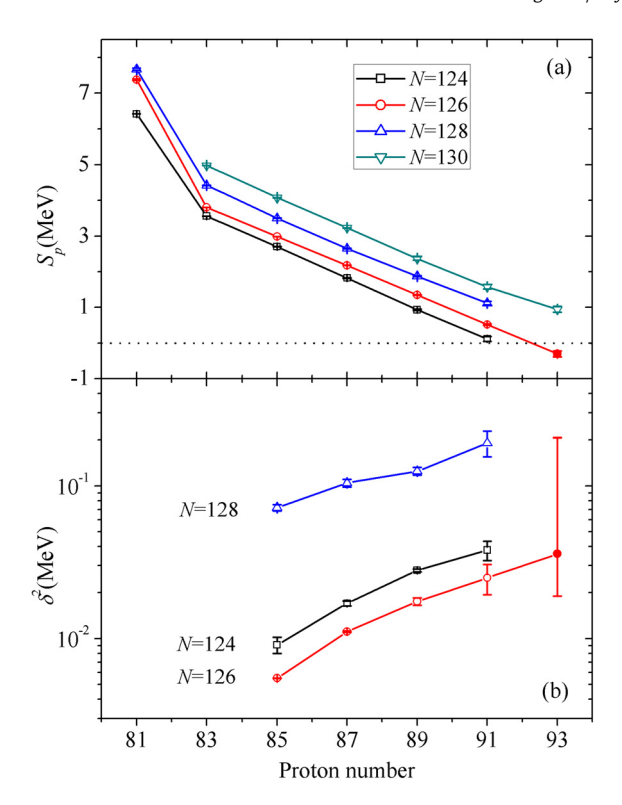


**Fig. 4.** (Color online.) (a) Proton binding energies  $S_p$  of odd-Z Tl-Np isotopes and reduced  $\alpha$ -decay widths  $\delta^2$  [26] of odd-Z At-Np isotopes as a function of proton number. Proton binding energies of known isotopes were taken from Ref. [24]. The red solid circles refer to the values of  $^{219}$ Np deduced in present work.

does not exhibit any abrupt change between Z=91 and Z=93. Whereas an abrupt reduction of proton binding energies is seen between Z=81 and Z=83 due to the influence of Z=82 shell. This result gives another evidence that there is no sub-shell closure at Z=92. In Ref. [7], ground state binding energies relative to  $^{208}$ Pb were calculated using shell model for the N=126 isotones  $^{210}$ Po to  $^{220}$ Pu. The calculated binding energy of  $^{219}$ Np relative to  $^{208}$ Pb is  $^{289}$ 69 keV [7] and this theoretical value is in agreement with the experimental value of  $^{289}$ 28(81) keV.

A spin-parity of  $(9/2^{-})$  is tentatively assigned to the ground state of <sup>219</sup>Np based on the large-scale shell model calculations [7]. Assuming  $\Delta L = 0$ , the reduced  $\alpha$ -decay width  $\delta^2(^{219}\text{Np}) =$  $36^{+171}_{-17}$  keV can be deduced for the 9039(40) keV decay using the Rasmussen approach [26]. In Ref. [1], the systematic regularities of  $\delta^2$  in even-Z Po-U isotopes were presented. Through the comparative analysis of the  $\alpha$ -decay reduced widths and the neutron-shell gaps of the Po-U isotopes, a significant weakening of influence of the N = 126 shell closure in U was observed. Here the new datum together with literature values allow us to construct the tendencies of  $\delta^2$  in odd-Z isotones up to Np. As shown in Fig. 4(b), this new datum extends smoothly the systematic regularities despite the large errors come from poor statistics. The smooth rise of  $\delta^2$ values with increasing proton number indicates that the weakening of the influence of N = 126 shell closure still effect for Np. But due to the large errors of the determined  $\delta^2$  value, significant statistics on <sup>219</sup>Np are needed to verify this inference.

As mentioned earlier, the first identification of  $^{219}$ Np has been reported in Ref. [3]. In that work  $^{219}$ Np was populated by the  $\alpha$  decay from the new isotope  $^{223}$ Am, which was produced in the multi-nucleon transfer reaction  $^{48}$ Ca+ $^{248}$ Cm and was separated by the velocity filter SHIP at GSI. The measured lifetime of  $^{223}$ Am was 7.5 ms. Due to the pileup of  $\alpha_1$  and  $\alpha_2$  in the observed decay chain, the lifetime of  $^{219}$ Np was not measured and only an es-

timated value of <5 µs was given. In addition, a lower limit of 9000 keV was estimated for the  $\alpha$ -particle energy of  $^{219}$ Np by assuming that the full energy of the  $\alpha_1$  was deposited in the stop detector and only  $\alpha_2$  escaped to the box detector. Because neither half-life nor decay energy was clearly measured, the identification of  $^{219}$ Np was not treated as a new nuclide by M. Thoennessen [27]. The  $\alpha$ -particle energy of  $^{219}$ Np measured in present work is consistent with the lower limit of the  $\alpha$ -particle energy of  $^{219}$ Np claimed in [3], but the measured lifetime is longer than what they claimed significantly. This inconsistent result maybe come from very poor statistics in both works. Therefore, further experiments are necessary to improve the decay properties of the semi-magic nucleus  $^{219}$ Np.

#### 5. Conclusion

In conclusion, we reported on the first measurement of the  $\alpha$ -decay properties of  $^{219}$ Np produced in the fusion reaction  $^{36}$ Ar+ $^{187}$ Re. The  $\alpha$ -particle energy of 9039(40) keV and half-life of  $0.15^{+0.72}_{-0.07}$  ms were extracted by using digital algorithms. According to the  $\alpha$ -particle energy, a proton binding energy of -301(83) keV was determined for  $^{219}$ Np and this new datum fits well into the systematics, which gives another evidence of that there is no subshell closure at Z=92. Negative value of proton binding energy indicates that  $^{219}$ Np is a semi-magic nucleus beyond the proton drip-line. The analysis of the reduced widths shows that the weakening of the influence of the N=126 shell closure maybe still exist in Np.

#### Acknowledgements

The authors would like to thank the HIRFL accelerator staff for delivering stable beams of high intensity. In addition, they acknowledge H.Q. Zhang for his useful discussions and critical reading of the manuscript and X.T. He for her theoretical support in the shell model calculation. This work is supported in part by the National Natural Science Foundation of China under Grant Nos. 11405225, 11475226, 11661131003, 11605250, 11605268, 11405243, 11535004, 11375086 and the National Basic Research Program of China under Grant No. 2013CB834403.

#### References

- [1] J. Khuyagbaatar, A. Yakushev, Ch.E. Düllmann, et al., New short-lived isotope  $^{221}$ U and the mass surface near N=126, Phys. Rev. Lett. 115 (2015) 242502.
- [2] M.D. Sun, Z. Liu, T.H. Huang, et al., New short-lived isotope  $^{223}$ Np and the absence of the Z=92 subshell closure near N=126, Phys. Lett. B 771 (2017) 303–308.
- [3] H.M. Devaraja, S. Heinz, O. Beliuskina, et al., Observation of new neutron-deficient isotopes with  $Z \ge 92$  in multinucleon transfer reactions, Phys. Lett. B 748 (2015) 199–203.
- [4] S. Heinz, H.M. Devaraja, O. Beliuskina, et al., Synthesis of new transuranium isotopes in multinucleon transfer reactions using a velocity filter, Eur. Phys. J. A 52 (2016) 278.
- [5] Z.Y. Zhang, L. Ma, Z.G. Gan, et al., A gas-filled recoil separator, SHANS, Nucl. Instrum. Methods B 317 (2013) 315–318.
- [6] K. Rutz, M. Bender, P.-G. Reinhard, et al., Odd nuclei and single-particle spectra in the relativistic mean-field model, Nucl. Phys. A 634 (1998) 67–88.
- [7] E. Caurier, M. Rejmund, H. Grawe, Large-scale shell model calculations for the N = 126 isotones Po-Pu, Phys. Rev. C 67 (2003) 054310.
- [8] K. Hauschild, M. Rejmund, H. Grawe, et al., Isomer spectroscopy in <sup>216</sup><sub>90</sub>Th<sup>126</sup> and the magicity of <sup>218</sup><sub>92</sub>U<sup>126</sup>, Phys. Rev. Lett. 87 (2001) 072501.
- [9] A.-P. Leppänen, J. Uusitalo, S. Eeckhaudt, et al., Alpha-decay study of  $^{218}$ U; a search for the sub-shell closure at Z=92, Eur. Phys. J. A 25 s01 (2005) 183–184
- [10] A.P. Leppänen, J. Uusitalo, M. Leino, et al.,  $\alpha$  decay studies of the nuclides  $^{218}$ U and  $^{219}$ U, Phys. Rev. C 75 (2007) 054307.

- [11] J.F. Ziegler, M.D. Ziegler, J.P. Biersack, SRIM the stopping and range of ions in matter (2010), Nucl. Instrum. Methods B 268 (2010) 1818–1823.
- [12] V1724&VX1724 User manual, Home/Products/Modular Pulse Processing Electronics/Waveform Digitizers/Digitizer Families/724 Digitizer Family, http://www.caen.it/, 2017. (Accessed 8 July 2017).
- [13] V.T. Jordanov, G.F. Knoll, Digital synthesis of pulse shapes in real time for high resolution radiation spectroscopy, Nucl. Instrum. Methods A 345 (1994) 337–345.
- [14] Z. Guzik, T. Krakowski, Algorithms for digital  $\gamma$ -ray spectroscopy, Nukleonika 58 (2013) 333–338.
- [15] R. Brun, F. Rademakers, ROOT an object oriented data analysis framework, Nucl. Instrum. Methods A 389 (1997) 81–86.
- [16] M. Cromaz, V.J. Riot, P. Fallon, et al., A digital signal processing module for gamma-ray tracking detectors, Nucl. Instrum. Methods A 597 (2008) 233–237.
- [17] K. Eskola, P. Kuusiniemi, M. Leino, et al.,  $\alpha$  decay of the new isotope  $^{206}$ Ac, Phys. Rev. C 57 (1998) 417–419.
- [18] C.M. Folden, Development of Odd-Z-Projectile Reactions for Transactinide Element Synthesis, PhD thesis, University of California, 2004, UMI number: 3167194.

- [19] F.P. Heßberger, S. Hofmann, D. Ackermann, et al., Decay properties of neutron-deficient nuclei in the region Z=86-92, Eur. Phys. J. A 8 (2000) 521–535.
- [20] Chart of nuclides, http://www.nndc.bnl.gov/chart, 2017. (Accessed 17 July 2017).
- [21] K.-H. Schmidt, C.-C. Sahm, K. Pielenz, H.-G. Clerc, Some remarks on the error analysis in the case of poor statistics, Z. Phys. A 316 (1984) 19–26.
- [22] Y.J. Ren, Z.Z. Ren, New Geiger–Nuttall law for  $\alpha$  decay of heavy nuclei, Phys. Rev. C 85 (2012) 044608.
- [23] Y.J. Ren, Z.Z. Ren, New Geiger–Nuttall law of odd–Z nuclei and long-lived island beyond the stable line, Nucl. Sci. Tech. 24 (2013) 050518.
- [24] M. Wang, G. Audi, F.G. Kondev, et al., The AME2016 atomic mass evaluation (II). Tables, graphs and references, Chin. Phys. C 41 (2017) 030003.
- [25] Z.G. Gan, J. Jiang, H.B. Yang, et al.,  $\alpha$  decay studies of the neutron-deficient uranium isotopes <sup>215–217</sup>U, Chin. Sci. Bull. 61 (2016) 2502–2511 (in Chinese).
- [26] J.O. Rasmussen, Alpha-decay barrier penetrabilities with an exponential nuclear potential: even-even nuclei, Phys. Rev. 113 (1959) 1593-1598.
- [27] M. Thoennessen, 2015 update of the discoveries of nuclides, Int. J. Mod. Phys. E 25 (2016) 1630004.